

# Introducing a new generation multi-sensor airborne system for mapping sea ice cover of polar oceans

Andreas A. Pfaffhuber,<sup>1\*</sup> Stefan Hendricks,<sup>2</sup> Priska Hunkeler<sup>2</sup> and Yme A. Kvistedal<sup>1</sup> present MAiSIE (Multi-sensor, Airborne Sea Ice Explorer), a new generation of helicopter-electromagnetic (HEM) ice thickness mapping technology to overcome the limitations of current systems which are restricted to 1D interpretation due to common procedures and systems mainly sensitive to layered structures.

One of the key data sets for climate studies is sea ice volume and its inter-annual variation. Helicopter electromagnetic (HEM) surveys have been playing an increasing role in this field being the only geophysical method capable of directly measuring ice thickness. With the work we present here, we strive to improve the versatility and accuracy of such systems.

Regional mapping of sea ice thickness distribution using HEM began in the late eighties in North America with traditional exploration systems later leading to sea ice dedicated devices (Kovacs and Holladay, 1990). Since the new millennium, purpose developed, digital sea ice HEM systems have been used on an operational basis during ship- and land-based expeditions in the Arctic, Antarctic, and Baltic seas (Haas et al., 2008).

Detailed studies on the accuracy of airborne EM (AEM) ice thickness data have revealed certain limitations. Several authors have addressed the effect of bird motion (attitude) both for AEM in general but also for sea ice AEM (Holladay and Prinsenberg, 1997). Traditional systems don't measure pitch and roll, making it impossible to correct for attitude errors. Further, standard one-dimensional (1D) data processing tends to underestimate ice thickness for non-1D regions such as pressure ridges. 3D modelling shows that ridge thickness may be under-estimated by up to 50% (Hendricks

2009). 3D inversion of horizontal coplanar (HCP) data provided by traditional systems result in minor improvements, as the HCP configuration is mostly sensitive to horizontally layered structures. Further EM orientations are needed as input data for 2D or 3D interpretation (Reid et al., 2003).

Based on the considerations above, we present a new generation system, the Multi-sensor Airborne Sea Ice Explorer (MAiSIE, Figures 1 & 2). MAiSIE comprises a multi-frequency and multi-component EM induction system accompanied by high-accuracy attitude sensors and three on-board laser devices (altimeter, IR thermometer, and 3D scanner, Figure 2 and Table 1). We believe that MAiSIE has the potential

Existing ice-HEM systems			
1-2 frequencies	HCP	altimeter	passive bucking

↓

MAiSIE			
broadband 500 Hz - 8 kHz	HCP, whale- and fishtail	altimeter, scanner, INS	active, digital bucking

Figure 1 Overview of specification upgrades with reference to European state of practice, such as systems owned by the Alfred Wegener Institute (AWI).

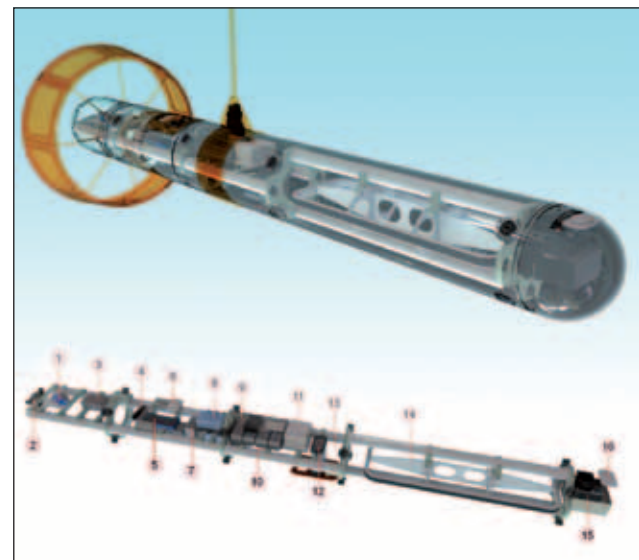


Figure 2 Design drawing showing main MAiSIE system components. (1) calibration coil, (2) EM receiver coils, (3) Rx amplifiers, (4) Dual dGPS receiver, (5) Digital data acquisition and EM controller, (6 & 16) GPS antenna, (7) Single board computer, (8) AC/DC converters, (9) EM transmitter power supply, (10) Space for laser scanner, (11) INS, (12) Laser altimeter, (13) Space for IR thermometer, (14) EM transmitter loop, and (15) EM transmitter amplifier.

<sup>1</sup> Norwegian Geotechnical Institute, PO Box 3930 Ullevål Stadion, 0806 Oslo, Norway.

<sup>2</sup> Alfred Wegener Institute for Polar and Marine Research, Bussestr. 24, 27570 Bremerhaven, Germany.

\* Corresponding author, E-mail: aap@ngi.no

## Near Surface Geoscience



Figure 3 MAiSIE at high altitude close to Barrow Alaska. Photo courtesy David Ball.

to initiate a second generation of sea ice EM-systems and will improve the quality of AEM derived sea ice thickness estimates significantly.

### Sea ice thickness as a geophysical target

The basic principle of HEM sea ice thickness profiling is to estimate the distance to the ice/water interface from the EM data, while a laser altimeter in the towed instrument (EM-bird) determines the system height above the ice or snow surface. The difference of these two distances consequently

corresponds to the ice (or ice + snow) thickness. We provided a detailed description and discussion of AEM ice thickness retrieval in Pfaffling et al. (2007) and Haas et al. (2009).

Pressure ridges are porous, blocky structures formed in deformation events, when two convergent ice floes break due to lateral stress. These ridges, which may exceed thicknesses of 25 m, contribute to the thickest sea ice in ice-covered seas and present a hazard for commercial operations. They also govern the stability of the land-fast sea ice zone close to the coast when grounded ridges and their blocky structures result in a large ice-water interface, which might trigger ice melting in summer. The state of practice HEM sea ice data processing is strictly one-dimensional, leading to a general thickness under-estimation of 2D or 3D structures such as pressure ridge by at least 50% (Reid et al. 2003). 3D modelling results showed that the under-estimation of the thickness of so-called pressure ridges is significant and variable over a range of 20–50% (Hendricks 2009). These results are consistent with findings in the field based on drilling profiles (Pfaffling et al., 2007) that traditional HEM systems are not capable of resolving the maximum thickness of pressure ridges and their porosity. Thus, an enhanced HEM ice thickness retrieval is needed to enable the investigation of the role of pressure ridges in the open sea and shallow coastal waters.

### EM concept

The EM system stands out with three main details outlined in Table 2: A multi-frequency signal, a receiver coil triplet, and active cancelling of the primary field. Based on the latter we can apply real-time EM processing following Equation 1, providing calibrated and zeroed normalized secondary field  $Z$

$$Z = \frac{H_z}{H_p} = cal \frac{R - cT}{cT} \quad (1)$$

Physical data	Length 3.5 m, weight 100 kg
EM system	Multi frequency system 500 Hz–8 kHz, freely programmable One transmitter loop for all frequencies, current feedback transmitter amplifier, active digital bucking, on-board calibration Coil geometries horizontal coplanar, fish tail and whale tail (vertical dipole transmitter, three-axis receiver) Coil separation: 2.65 m (Hz, Hx), 2.68 m (Hy)
Auxiliary sensors	Laser altimeter (Riegl LD 90) Inertial Navigation System (INS) combined with dual antenna differential GPS (Novatel SPAN CPT & FlexPac-G2) Prepared for laser scanner (Riegl VQ580) and IR ground surface thermometer (Heitronics KT19) On-board data acquisition (NI cRIO real-time controller and FPGA & single board computer)
Operational details	Towing cable length 20 or 30 m Bird altitude 10–15 m above ice surface, speed 60–80 knots (30–40 m/s) System powered by helicopter power supply 400 W @ 28 VDC System controlled by operator laptop via towing cable or WLAN

Table 1 Detailed list of MAiSIE's system components.

Multifrequency transmitter	The transmitted signal follows a multi-frequency concept, similar to Geophex’s GEM-2A system. A time series composed of several frequencies in a range from 500 Hz–8 kHz is fed through the transmitter loop with a moment of 6 to 25 Am <sup>2</sup> (NIA).
3-axis receiver	A triplet of lightweight ferrite core coils acquires the secondary field in all room directions. This sensor was developed in cooperation with CNRS/Paris, based on a space-borne magnetometer developed by this group.
Dynamic, active bucking	We sample the transmitted EM field directly on the transmitter loop and use this signal to actively cancel (zeroing or bucking) the primary field by virtue of a second set of windings integrated in the receiver coils, creating an active bucking at the receiver location. This digital bucking is adjusted for every production flight during a bucking and calibration sequence at high altitude. As we monitor the transmitted current directly on the Tx loop, we can dynamically zero the primary field response and thus minimize drift due to Tx instabilities.

Table 2 EM concept.

with  $H_p$  being the primary (field in a non-conductive full-space) and  $H_s$  the secondary magnetic field strength (field above a conductive space arising from the eddy currents induced by the primary field).

The sampled voltage on the receivers and the transmitter current are expressed as  $R$  and  $T$ , respectively. The system’s transfer function  $c$  is determined at high altitude where  $H_s$  must be zero and thus  $c=R/T$ . Finally, the calibration factor  $cal$  is applied to account for all remaining uncertainties, such as inaccuracies in loop size and shape, dimensions, and gain settings. The correct value for  $cal$  is established during calibration flights over deep water with known conductivity (Figure 4). This fundamental system calibration is controlled during every flight by virtue of the on-board calibration coil, providing a known secondary field at the receivers. All variables leading to the normalized secondary field in Equation 1

are complex numbers required separately for each active signal frequency and for each of the three receiver components.

Data quality

The performance of the EM system was evaluated on 1 December 2011 during a proof-of-concept test flight over the North Sea close to the German island of Helgoland with the primary focus on noise, drift, and calibration assessments. The chosen multi-frequency configuration included four frequencies (0.5, 1.01, 4.1, and 7.95 kHz), with 4.1 kHz as the main frequency of interest (Figure 4). In Pfaffhuber et al. (2012) we discuss these tests in full detail. The measured data agrees well with forward-modelled responses assuming a 4 S/m ocean water conductivity (typical for this area and season). High altitude noise tests revealed a standard deviation of 20 ppm for the 4.1 kHz in-phase channel,

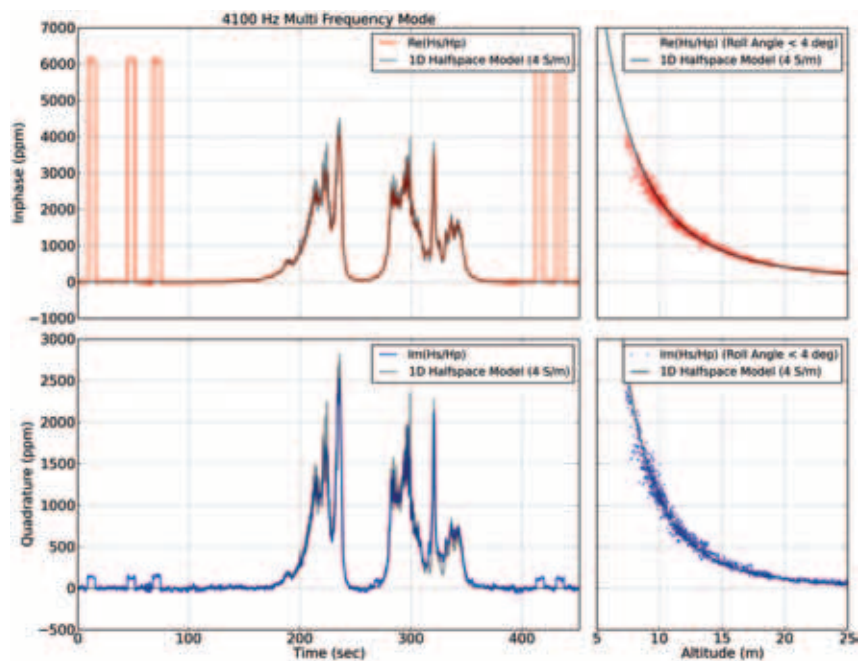


Figure 4 Calibrated and modelled EM response over water (z-component only) given by in-phase (top, red) and quadrature (bottom, blue) channels at 4.1 kHz. The panels on the left hand side show the comparison of measured and modelled data along the profile, on the right hand the side the comparison is given as a function of instrument height above the water.

# Near Surface Geoscience

leading to a derived ice thickness uncertainty of 10 cm at a system altitude of 13 m. As 10 cm are the desired ice thickness accuracy, we grew confident enough to move on to first ice trials in early 2012. The lower frequencies, however, showed higher noise levels and noise reducing measures are subject of our ongoing research (Pfaffhuber et al., 2012).

A first full-scale field trial was carried out with helicopter surveys over sea ice in the Beaufort Sea near Barrow Alaska

in April 2012 during the NSF-funded Seasonal Ice Zone Observation Network (SIZONet) field campaign. Sea ice in the Beaufort Sea is characterized by a mix of young and old ice, as well as heavy deformation zones near the coast line. The properties of the near-shore deformed ice are important for the socio-economic use of the landfast sea ice, while the spring thickness of drifting sea ice further offshore determines the chance of survival in the following summer.

Calibration with 1D Forward Model (z - component)

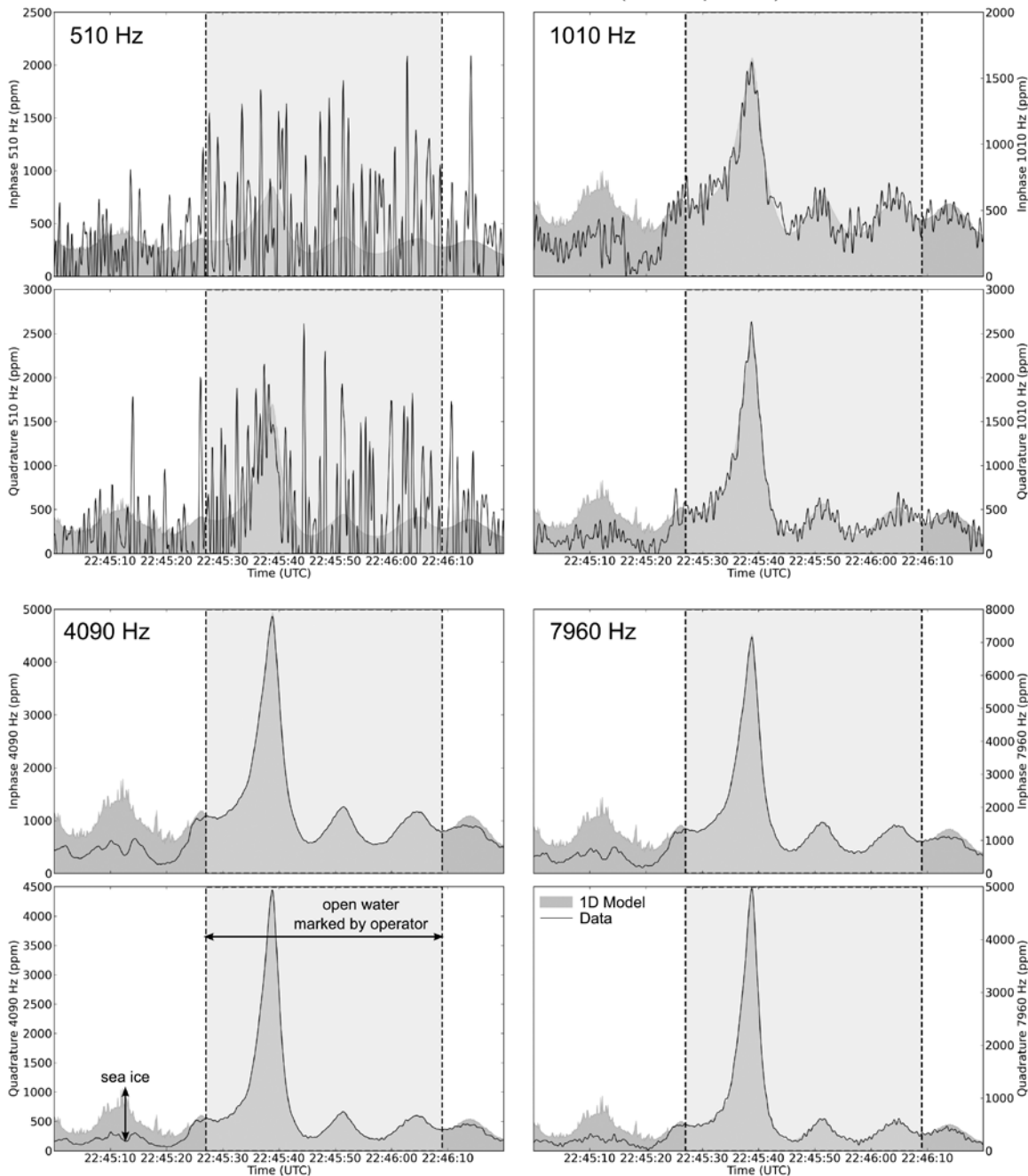
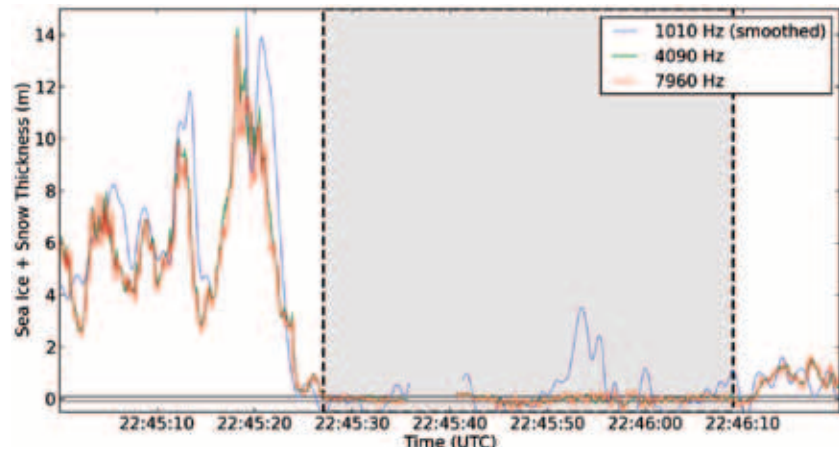


Figure 5 Calibrated EM data over sea ice for four frequencies showing in-phase (top panels) and quadrature (bottom panels) components. The section shows a roughly 500 m long profile with sea ice and open water, manually marked by the operator.



**Figure 6** Ice thickness estimates derived from data segment shown in Figure 5 with a 1D interpretation of each frequency. The 500 Hz frequency was omitted due to insufficient signal to noise for sea ice thickness estimation. The vertical lines indicate open water, the horizontal lines, the +/- 10 cm error level over open water.

One goal of SIZONet is to characterize the ice thickness distribution in the seasonal ice zone of the Beaufort Sea to assist short-term ice forecasting.

The field programme consisted of four flights which were used for general ice thickness classification and a MAiSIE capability test for deformed sea ice. Some surveys were flown together with other airborne missions to achieve a common dataset with multiple sensors, such as radar and laser altimeters and airborne synthetic aperture radar. The helicopter thickness surveys had significantly longer flight times (> 2 hours) than the first instrument tests over the North Sea in December 2011. Each survey consisted of 20 minute-long drift and noise tests at high altitude over land in the beginning and end of each flight. Air temperatures around -20°C and ambient temperature changes in the order of several degrees resulted in significant and non-linear sensor drift. A first visual inspection reveals a good correlation of sensor drift and temperature recording at the receiver coils at high altitude, motivating temperature-based correction.

Strong westerly winds caused several openings in the ice cover with sizes ranging from hundred of metres to several kilometres. The smaller openings showed very little surface waves, which makes them an ideal target for calibration of the system. The upper Arctic Ocean is typically mixed to a depth of several tens of metres with a constant electrical conductivity of 2.4 S/m, hence this openings form ideal 1D cases for the frequencies used.

Figure 5 shows the comparison of a 1D forward model-based on the laser range data and the calibrated z-component of all MAiSIE frequencies (510 Hz, 1010 Hz, 4090 Hz, and 7960 Hz). The shaded area shows the extent of the open water which was manually marked by the operator in the helicopter. The spatial extent of the section shown is roughly 500 m. Corrections of the laser range based on the actual attitude of the sensor, measured by the INS are not included. The measured signal and the forward models closely agree over open water. The agreement is even better than the test over the North Sea (Figure 4), probably due to the absence

of surface waves. Over sea ice the forward model deviates significantly from the measured data as one expects.

The two higher frequencies (4090 and 7960 Hz) are in close agreement with the 1D forward models. The two lower frequencies (510 and 1010 Hz) suffer from higher noise levels, however first improvements were made by fine tuning frequencies after the test flight over the North Sea.

A 1D interpretation of the Inphase-component of each frequency by direct inversion (Pfaffling et al., 2007 and Haas et al., 2009) was used to calculate ice thickness and to illustrate the accuracy of the system (Figure 6). The 500 Hz frequency was omitted due to the insufficient signal to noise level as the frequency is not suitable for ice thickness retrieval but rather bathymetry surveying. The 1010 Hz EM data was low-pass filtered (Hamming filter) to suppress high-frequency noise. The comparably low sensitivity and higher noise level on the lower frequency is visible over open water, falsely indicating ice thicknesses up to 2 m. The two higher frequencies are mostly within the +/- 10 cm error level over open water (marked as horizontal lines). Over sea ice they also give very comparable thickness results. Small lateral differences are evident, which motivate more accurate ice thickness retrieval with a 2D or 3D interpretation.

1D ice thickness data from all flights was calculated and released shortly after the campaign for the Study of Environmental Arctic Change (SEARCH) to assist local ice forecasting for summer 2012.

**Discussion**

Test flights in December 2011 revealed the capabilities of a multi-frequency and multi-component EM configuration, but also showed room and need for further optimization. The comparably small coil spacing (2.65 m) is a major challenge compared to large exploration systems in terms of noise level. The small and light bird can, however, be flown two to three times lower than big and heavy systems and thus opens opportunities for higher lateral resolution due to the reduced footprint. First data over sea ice confirm our positive expectations

## Near Surface Geoscience

and provide first indications of the desired frequency depending lateral resolution. Formal 2D or 3D inversion of the data is needed to gain the full value of the multi-component data, and adequate algorithms are under development.

### Acknowledgments

We thank AWI and NGI for funding and permission to publish. MAiSIE would not exist without the enthusiasm and expertise of the NGI project team: Yme Kvistedal, Erik Lied, Ivar-Kristian Waarum, Philip Hayes, supported by Mathieu Boda, Ole-Espen Buer, Stephen Hayes, Harald Iwe, Pawel Jankowski, Matthew J Lato, Frank Myrvoll, Ole Petter Rotherud, James M Strout and Inge Viken. Christophe Coillot contributed with his group's expertise for the EM receiver. Figures 2 and 4 are reproduced courtesy of SEG copyright. Field work has been supported by HeliService International and ERA Helicopters as well as Andy Mahoney, Hajo Eicken, and the SIZONet campaign funded by the US National Science Foundation.

### References

Haas, C., Pfaffling, A., Hendricks, S., Rabenstein, L., Etienne, J.-L. and Rigor, I. [2008] Reduced ice thickness in Arctic Transpolar Drift favors rapid ice retreat. *Geophysical Research Letters*, 35, L17501.

Haas, C., Lobach, J., Hendricks, S., Rabenstein, L. and Pfaffling, A. [2009] Helicopter-borne measurements of sea ice thickness, using a small and lightweight, digital EM bird. *Journal of Applied Geophysics*, 67, 234–241.

Hendricks, S. [2009] *Validation of altimetric sea ice thickness measurements with a helicopter based electromagnetic induction method*. PhD thesis (in German), University of Bremen, Germany.

Holladay, J. S. and Prinsenber S. K. [1997] Bird orientation effects in quantitative airborne electromagnetic interpretation of Pack Ice Thickness Sounding. *Oceans '97 Marine Technology Society Institute of Electrical and Electronic Engineers Conference*, 2, 1114–1116.

Kovacs, A. and Holladay J. S. [1990] Sea ice thickness measurement using a small airborne electromagnetic sounding system. *Geophysics*, 55, 1327–1337.

Pfaffhuber, A. A., Hendricks, S. and Kvistedal, Y. [2012] Progressing from 1D to 2D and 3D near surface airborne electromagnetic mapping with a multi-sensor airborne sea ice explorer. *Geophysics*, 77(4), in press.

Pfaffling, A., Haas C. and Reid J. E. [2007] A direct helicopter EM sea ice thickness inversion, assessed with synthetic and field data. *Geophysics*, 72, F127–F137.

Reid, J. E., Vrbancich J., and Worby A. P. [2003] A comparison of shipborne and airborne electromagnetic methods for Antarctic sea ice thickness measurements: *Exploration Geophysics*, 34, 46–50.

**Petrel**  
E&P SOFTWARE PLATFORM

#### See previously unseen details to discover new hydrocarbons

Interpret prestack data, project ray paths, and iteratively process depth volumes to characterize complex geometries in the subsurface—in context with all available data in the industry-leading Petrel\* E&P software platform.

Exploration teams can see more, do more, and understand more to confidently find new hydrocarbon resources.

Shared earth—critical insight.

[www.slb.com/petrel](http://www.slb.com/petrel)

**Schlumberger**